Second International Conference on
SPace, Aerospace & defenCE 2025

Paper Presentation

Paper id: #1571123857

Satellite Navigation and Control Using Discrete-APF and Fixed-Time Sliding Mode Controller

Author(s):

1. Paridhi D Choudhary
2. Rakesh Kumar Sahoo
3. Manoranjan Sinha

Contents

Rigid Body Dynamic Model of Target Satellite

The position, velocity and angular velocity of the target satellite in ECI frame is represented by $\tilde{r}_t$,$\tilde{v}_{tb}$ and $\widetilde{\Omega}_{tb}$and $\boldsymbol{R_{it}}$ represents the rotation matrix of target satellite wrt ECI frame.

The configuration of the target satellite on SE(3) manifold can be represented as 4×4 matrix

$$\boldsymbol{G}_t = \begin{bmatrix} \boldsymbol{R}_{it} & \tilde{r}_t \\ 0_{1\times 3} & 1 \end{bmatrix} \in SE(3) \qquad \textbf{(1)}$$

The unified velocity vector of the angular velocity and translational velocity of the target satellite can be represented by $\tilde{\xi}_{tb} = \left[\widetilde{\Omega}_{tb}\,, \tilde{v}_{tb}\right]^T \in \mathbb{R}^6$

The kinematics of the target satellite can be represented as $\dot{\boldsymbol{G}}_t = \boldsymbol{G}_t \tilde{\xi}_{tb}^{\vee}$ **(2)**

where $\tilde{\xi}_{tb}^{\vee}$ is the exponential mapping of $\tilde{\xi}_{tb} : \mathbb{R}^6 \to se(3)$

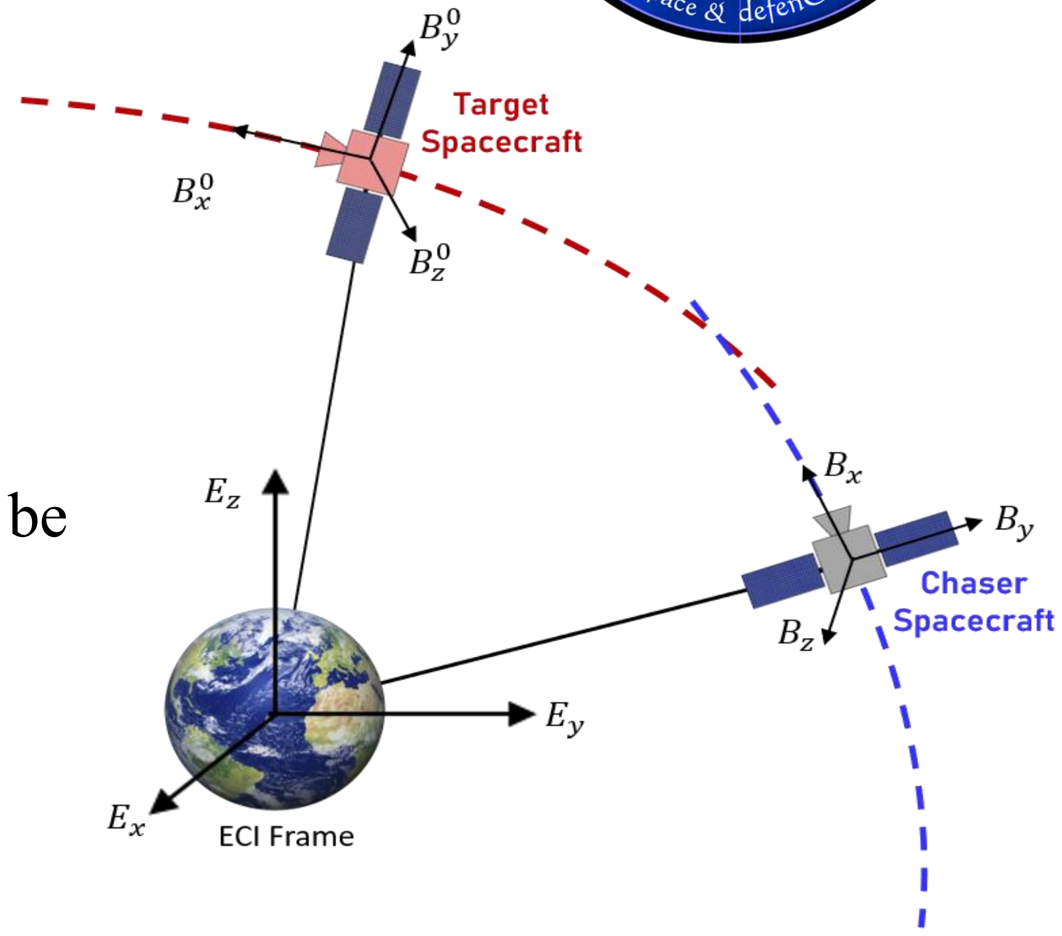

Fig. 1 Rendezvous and Docking maneuver of chaser satellite with the target satellite

Rigid Body Dynamic Model of Target Satellite

Let the unified matrix of mass and inertia of target satellite be represented as, $\mathbb{I}_t = \begin{bmatrix} \boldsymbol{J}_{tb} & 0_{3\times3} \\ 0_{3\times3} & m_t\boldsymbol{I}_3 \end{bmatrix} \epsilon\, \mathbb{R}^{6\times6}$

The coupled translational and rotational dynamics of the target satellite can be described using geometric mechanics as

$$\mathbb{I}_t\dot{\tilde{\xi}}_{tb} = ad^*_{\tilde{\xi}_{tb}}\mathbb{I}_t\tilde{\xi}_{tb} + \tilde{\varphi}_{tg} + \tilde{\varphi}_{td} \quad \textbf{(3)}$$

where

$\tilde{\varphi}_{tg}$ and $\tilde{\varphi}_{td}$ denotes the unified vector of gravitational force and gravity gradient torque, and the unified vector of external disturbance force and torque acting on the target satellite

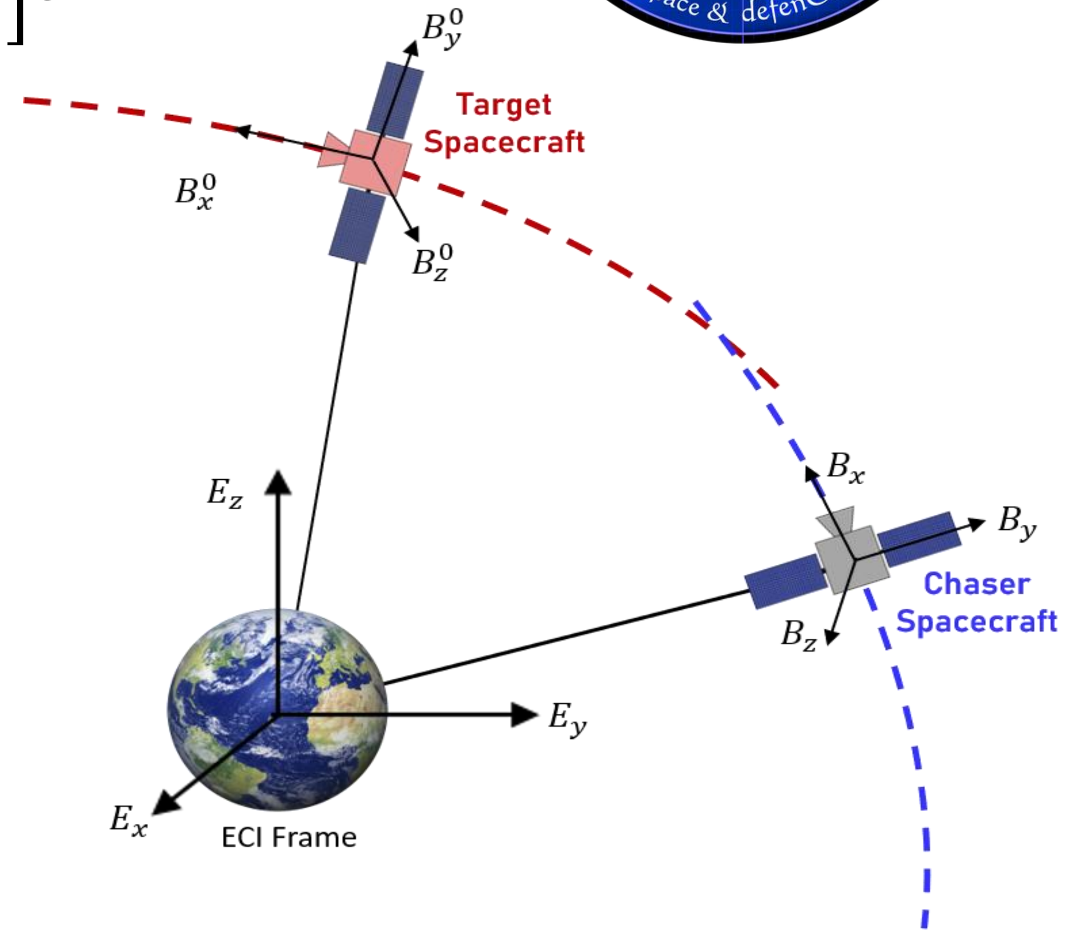

Fig. 1 Rendezvous and Docking maneuver of chaser satellite with the target satellite

Rigid Body Dynamic Model of Chaser Satellite

The position, velocity and angular velocity of the chaser satellite in ECI frame is represented by $\tilde{r}_c$,$\tilde{v}_{cb}$ and $\widetilde{\Omega}_{cb}$and $\boldsymbol{R_{ic}}$ represents the rotation matrix of chaser satellite wrt ECI frame.

The configuration of the chaser satellite on SE(3) manifold can be represented as 4×4 matrix

$$\boldsymbol{G}_c = \begin{bmatrix} \boldsymbol{R}_{ic} & \tilde{r}_c \\ 0_{1\times3} & 1 \end{bmatrix} \in SE(3) \qquad \textbf{(4)}$$

The unified velocity vector of the angular velocity and translational velocity of the chaser satellite can be represented by $\tilde{\xi}_{cb} = \left[\widetilde{\Omega}_{cb} , \tilde{v}_{cb}\right]^T \in \mathbb{R}^6$

The kinematics of the chaser satellite can be represented as $\dot{\boldsymbol{G}}_c = \boldsymbol{G}_c \tilde{\xi}_{cb}^{\vee}$ **(5)**

where $\tilde{\xi}_{cb}^{\vee}$ is the exponential mapping of $\tilde{\xi}_{cb} : \mathbb{R}^6 \rightarrow se(3)$

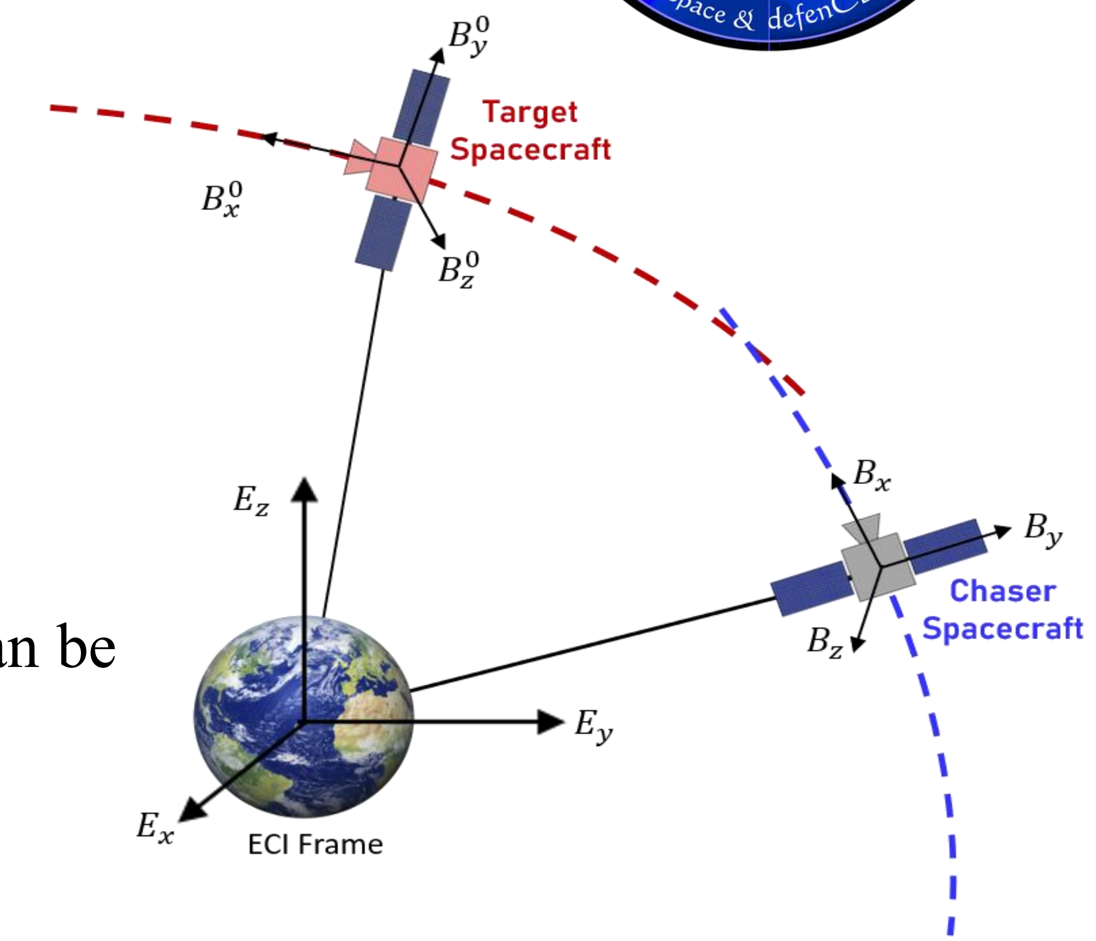

Fig. 1 Rendezvous and Docking maneuver of chaser satellite with the target satellite

Rigid Body Dynamic Model of Chaser Satellite

Let the unified matrix of mass and inertia of chaser satellite be represented as, $\mathbb{I}_c = \begin{bmatrix} \boldsymbol{J}_{cb} & 0_{3\times3} \\ 0_{3\times3} & m_c\boldsymbol{I}_3 \end{bmatrix} \in \mathbb{R}^{6\times6}$

The coupled translational and rotational dynamics of the target satellite can be described using geometric mechanics as

$$\mathbb{I}_c\dot{\tilde{\xi}}_{cb} = ad^*_{\tilde{\xi}_{cb}}\mathbb{I}_c\tilde{\xi}_{cb} + \tilde{\varphi}_{cc} + \tilde{\varphi}_{cg} + \tilde{\varphi}_{cd} + \tilde{\varphi}_{APF} \quad \textbf{(6)}$$

where

$\tilde{\varphi}_{cg}$ and $\tilde{\varphi}_{cd}$ denotes the unified vector of gravitational force and gravity gradient torque, and the unified vector of external disturbance force and torque acting on the chaser satellite; $\tilde{\varphi}_{cc}$ is the unified vector of external control torque and force acting on the chaser satellite body-fixed frame ; $\tilde{\varphi}_{APF}$ is the unified vector of external APF based torque and force acting on the chaser satellite

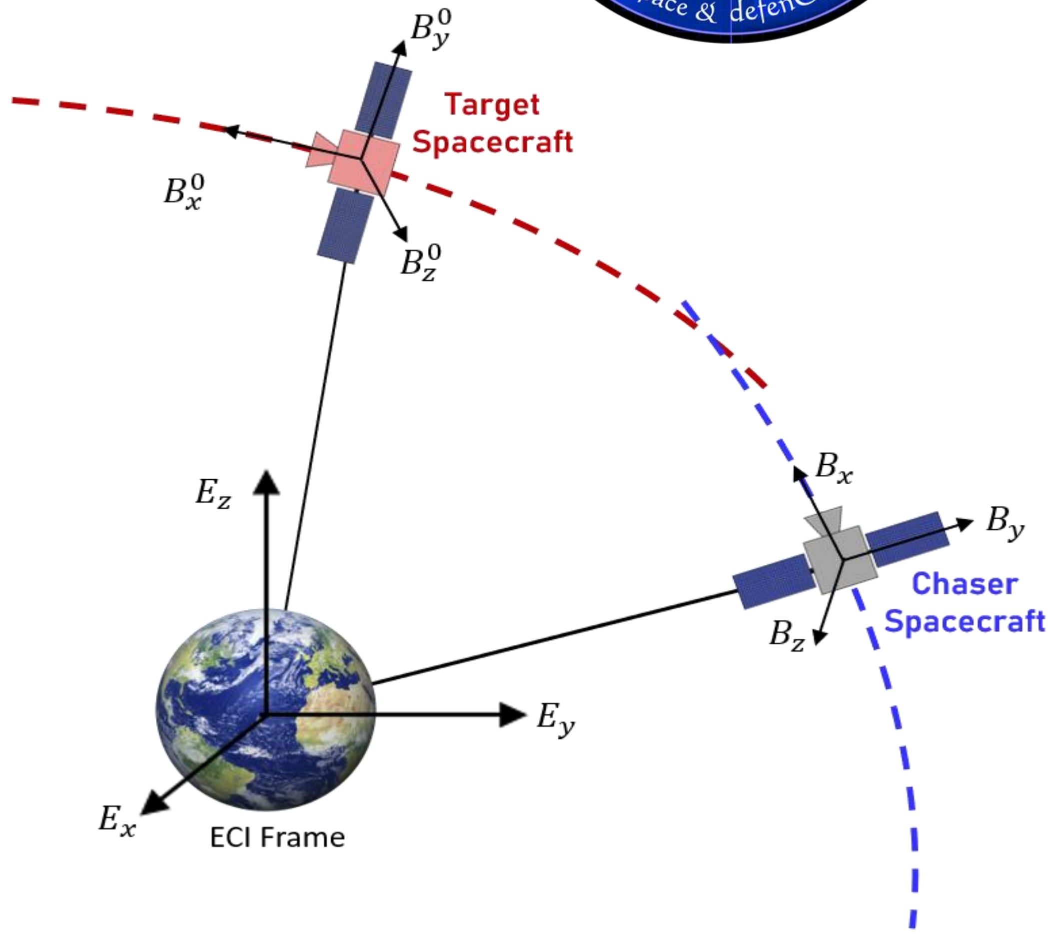

Fig. 1 Rendezvous and Docking maneuver of chaser satellite with the target satellite

Relative Kinematics and Dynamics of Satellite

Relative configuration : $\boldsymbol{H} = (\boldsymbol{G}_t)^{-1}\boldsymbol{G_c} \in SE(3)$

where the desired configuration : $\boldsymbol{G_{ct}} \in SE(3)$

The relative configuration tracking error vector $\tilde{\tau} = [\tilde{\gamma} \quad \tilde{b}]^T \in \mathbb{R}^6$ consisting of orientation tracking error $\tilde{\gamma}$ and position racking error $\tilde{b}$, is obtained by performing logarithmic mapping : $SE(3) \rightarrow se(3)$ as shown below.

$$\tilde{\tau}^{\vee} = logm(\boldsymbol{G_{ct}^{-1}} * H) \quad \textbf{(7)}$$

The relative velocity of the chaser satellite with respect to the target satellite in the chaser's body-fixed frame is expressed as

$$\tilde{\alpha} = \tilde{\xi}_{cb} - Ad_{\boldsymbol{H}^{-1}}\tilde{\xi}_{tb} \quad \textbf{(8)}$$

The relative dynamics of chaser satellite with respect to the target satellite is expressed as

$$\mathbb{I}_c\dot{\tilde{\alpha}} = \mathbb{I}_c\dot{\tilde{\xi}}_{cb} + \mathbb{I}_c\left(ad_{\tilde{\alpha}}Ad_{\boldsymbol{H}^{-1}}\tilde{\xi}_{tb} - Ad_{\boldsymbol{H}^{-1}}\dot{\tilde{\xi}}_{tb}\right) \quad \textbf{(9)}$$

$$\mathbb{I}_c\dot{\tilde{\alpha}} = \tilde{\varphi}_{cg} + \tilde{\varphi}_{cd} + \tilde{\varphi}_{cc} + \tilde{\varphi}_{APF} + \mathbb{I}_c\left(ad^*_{\tilde{\xi}_{cb}}\mathbb{I}_c\tilde{\xi}_{cb} + ad_{\tilde{\alpha}}Ad_{\boldsymbol{H}^{-1}}\tilde{\xi}_{tb} - Ad_{\boldsymbol{H}^{-1}}\dot{\tilde{\xi}}_{tb}\right) \quad \textbf{(10)}$$

Proposed Control Architecture

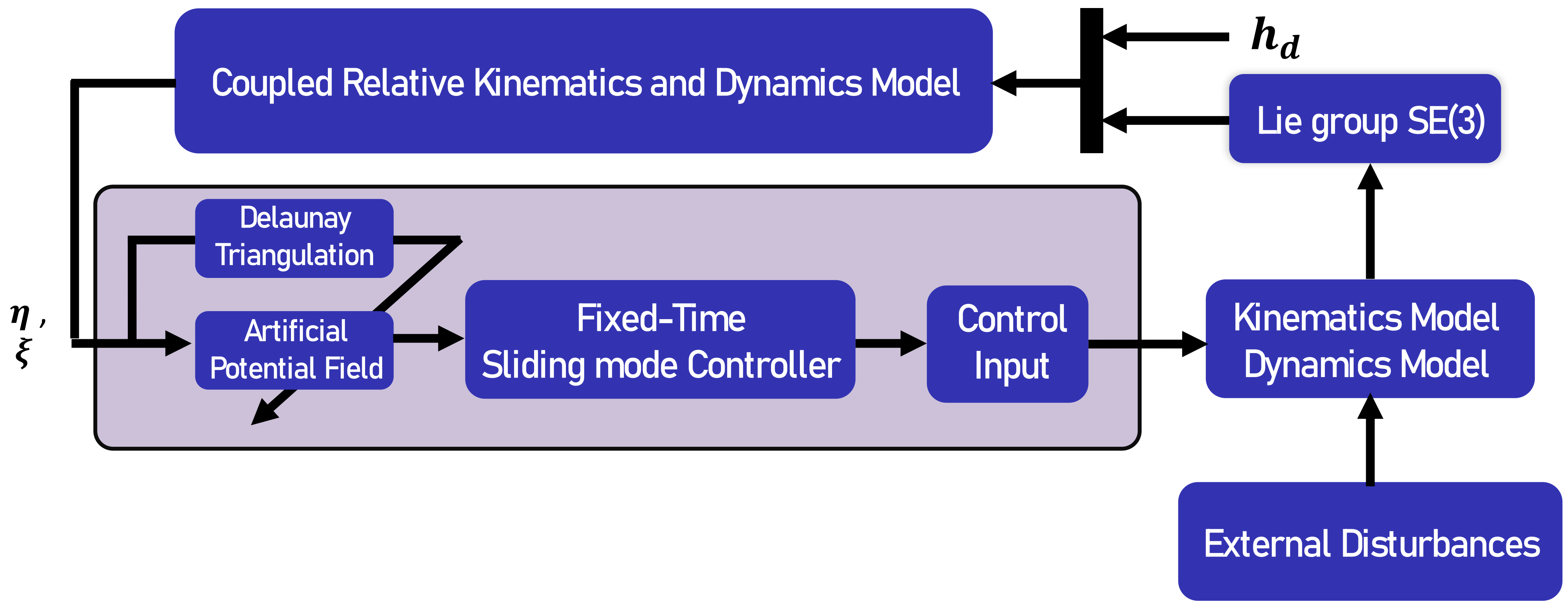

Fig. 2 Proposed architecture of collision-free path planning using Discrete APF and Fixed-Time SMC

Artificial Potential Field Algorithm

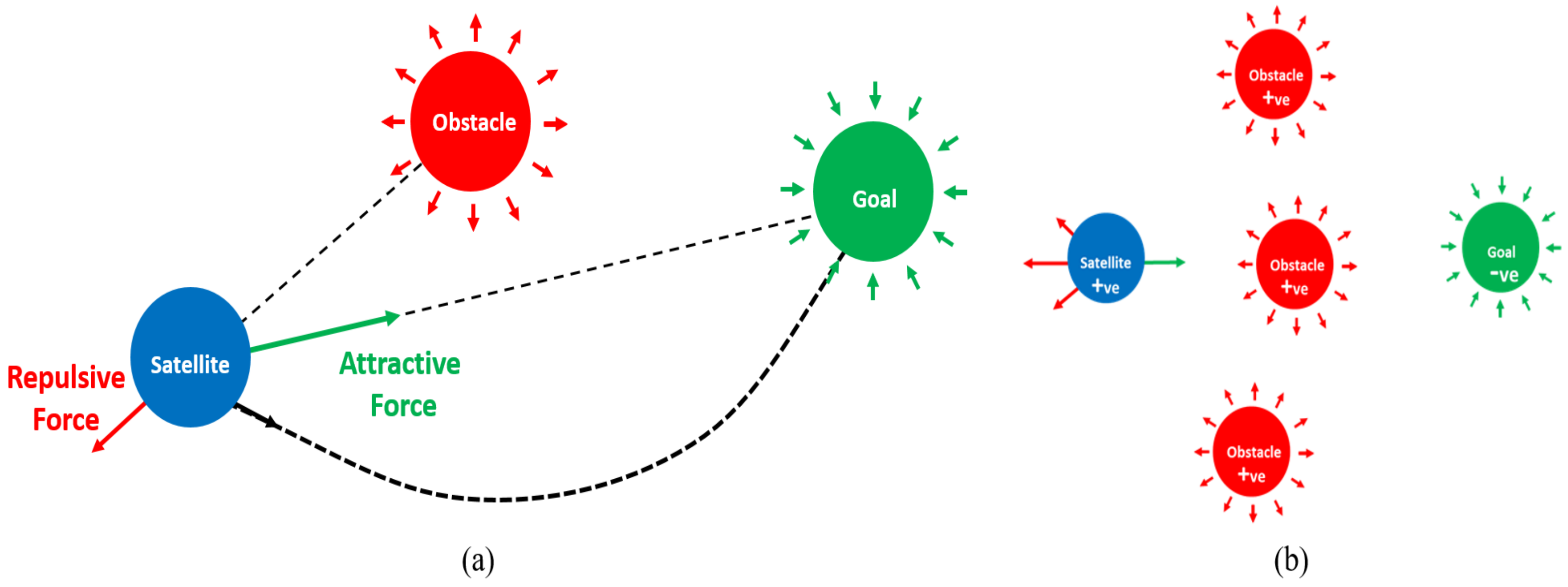

Fig. 3 Illustration of (a) Path planning using APF (b) Local minima scenario in presence of multiple obstacles

The expression of attractive potential is a quadratic function of relative position of chaser satellite w.r.t target satellite,

$$\tilde{U}_a = \frac{1}{2} k_a \left(\tilde{b}\right)^2$$

The expression of repulsive potential of obstacle as a function of relative position of chaser satellite w.r.t obstacle,

$$\tilde{U}_r = \frac{1}{2} k_r \left(\frac{1}{\tilde{b}_o}\right)^2$$

The resultant force $\tilde{F}_{APF}$ acting on the satellite is derived from the gradient of the respective potential function

$$\tilde{F}_{APF} = \nabla \tilde{U}_a + \nabla \tilde{U}_r$$

$$\tilde{F}_{APF} = \mathrm{k_a} \tilde{b} - \frac{k_r}{\left(\tilde{b}_o\right)^3}$$

Discrete - Artificial Potential Field Algorithm

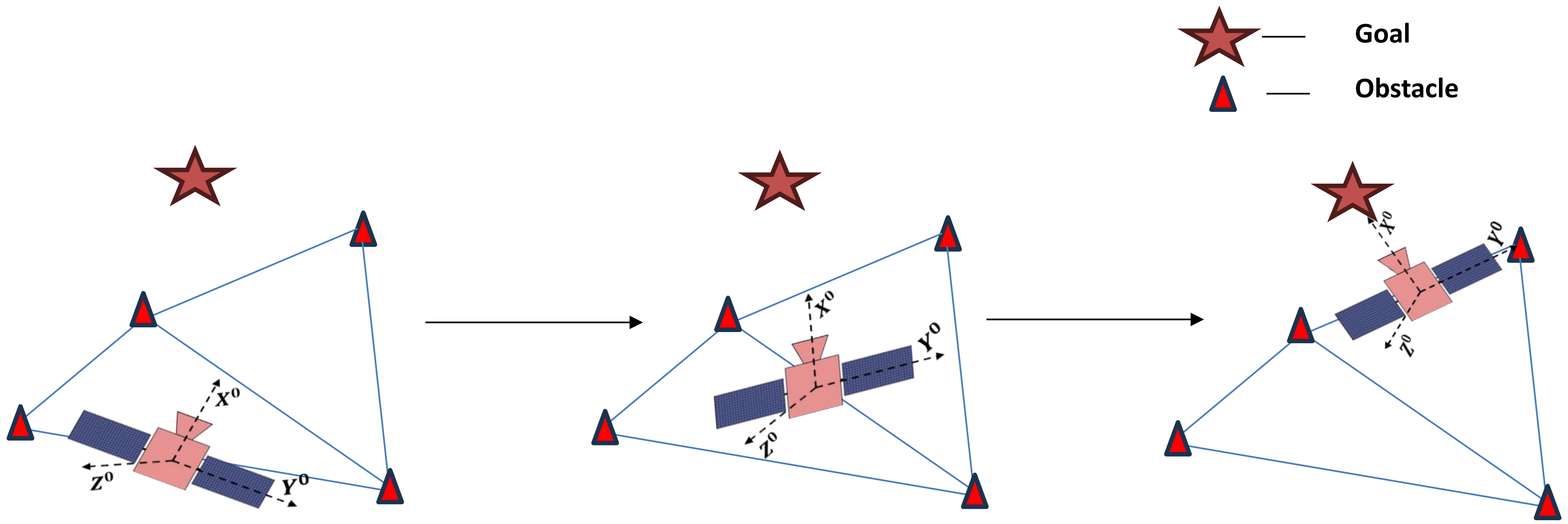

Fig. 4 Illustration of satellite motion through the obstacles using the proposed D-APF approach

Delaunay triangulation is a geometric-based approach used to divide a set of points in a plane into non-overlapping triangles, ensuring no other points lie within the circumcircle of each triangle.

Instead of considering the cumulative repulsive force from all obstacles, the algorithm focuses only on the two nearest obstacles at any instant determined using Delaunay triangulation based geometric method.

Fixed-Time Sliding Mode Controller

The fixed-time sliding surface consisting of the exponential coordinate vectors, $\tilde{b}$ and relative velocity, $\tilde{\gamma}$ to track the desired trajectory within fixed time is defined as

$$\tilde{s} = \tilde{\gamma} + \mathrm{k}_1 sig^{l_1}(\tilde{b}) + k_2 sig^{l_2}(\tilde{b}) \quad (11)$$

where
$\mathrm{k}_1, \mathrm{k}_2 > 0$, $0 < l_1 \leq 1$, $\mathrm{l}_2 > 1$, $\tilde{s} = [s_1, s_2, \dots, s_6] \epsilon\, \mathbb{R}^6$, $\tilde{\gamma} = [\gamma_1, \gamma_2, \dots, \gamma_6] \epsilon\, \mathbb{R}^6$ and $\tilde{\rho} = [b_1, b_2, \dots, b_6] \epsilon\, \mathbb{R}^6$.

A fixed-time reaching law based control law to ensure that the system states to reach the sliding surface within fixed time is defined as

$$\dot{\tilde{s}} = -\mathrm{k}_{s1} sig^{l_1}(\tilde{s}) - k_{s2} sig^{l_2}(\tilde{s}) \quad (12)$$

Consider the fixed time control input is defined as,

$$\begin{aligned} \tilde{\varphi}_{cc} = & -\tilde{\varphi}_{cg} - \tilde{\varphi}_{cd} - \tilde{\varphi}_{APF} - \mathbb{I}_c \Big(ad^*_{\tilde{\xi}_{cb}} \mathbb{I}_c \tilde{\xi}_{cb} + ad_{\tilde{\gamma}} Ad_{\boldsymbol{H}^{-1}} \tilde{\xi}_{tb} - Ad_{\boldsymbol{H}^{-1}} \dot{\tilde{\xi}}_{tb} \\ & + (\mathbb{Q}_1 + \mathbb{Q}_2) \boldsymbol{G}(\tilde{\boldsymbol{b}}) \tilde{\boldsymbol{\gamma}} \Big) - \mathrm{k}_{s1} sig^{l_1}(\tilde{s}) - k_{s2} sig^{l_2}(\tilde{s}) \end{aligned} \quad (13)$$

Fixed-Time Sliding Mode Controller

A continuous differentiable Lyapunov function is defined as, $V\left(\tilde{\sigma}, \tilde{\xi}_c, \boldsymbol{H}, \tilde{\xi}_t\right) = \frac{1}{2}\, \tilde{s}^T \mathbb{I}_c \tilde{s}$ **(14)**

Performing the time derivative of Lyapunov function and using the control input,

$$\dot{V}\left(\tilde{\sigma}, \tilde{\xi}_c, \boldsymbol{H}, \tilde{\xi}_t\right) = -k_{t1} V^{\frac{l_1+1}{2}} - k_{t2} V^{\frac{l_2+1}{2}} \tag{15}$$

where $k_{t1} = \left(2^{\frac{l_1+1}{2}}\right)\lambda_{min}(\mathrm{k}_{s1})$ and $k_{t2} = \left(2^{\frac{l_1+1}{2}}\right)\left(6^{\frac{l_2-1}{2}}\right) * \lambda_{min}(\mathrm{k}_{s2})$

Therefore, the system states will reach the desired sliding surface $\tilde{s} = 0$ within fixed-time, T_{max}

$$T \leq T_{max} = \frac{2}{k_{t1}(1 - l_1)} + \frac{2}{k_{t2}(l_2 - 1)} \tag{16}$$

Simulation Results

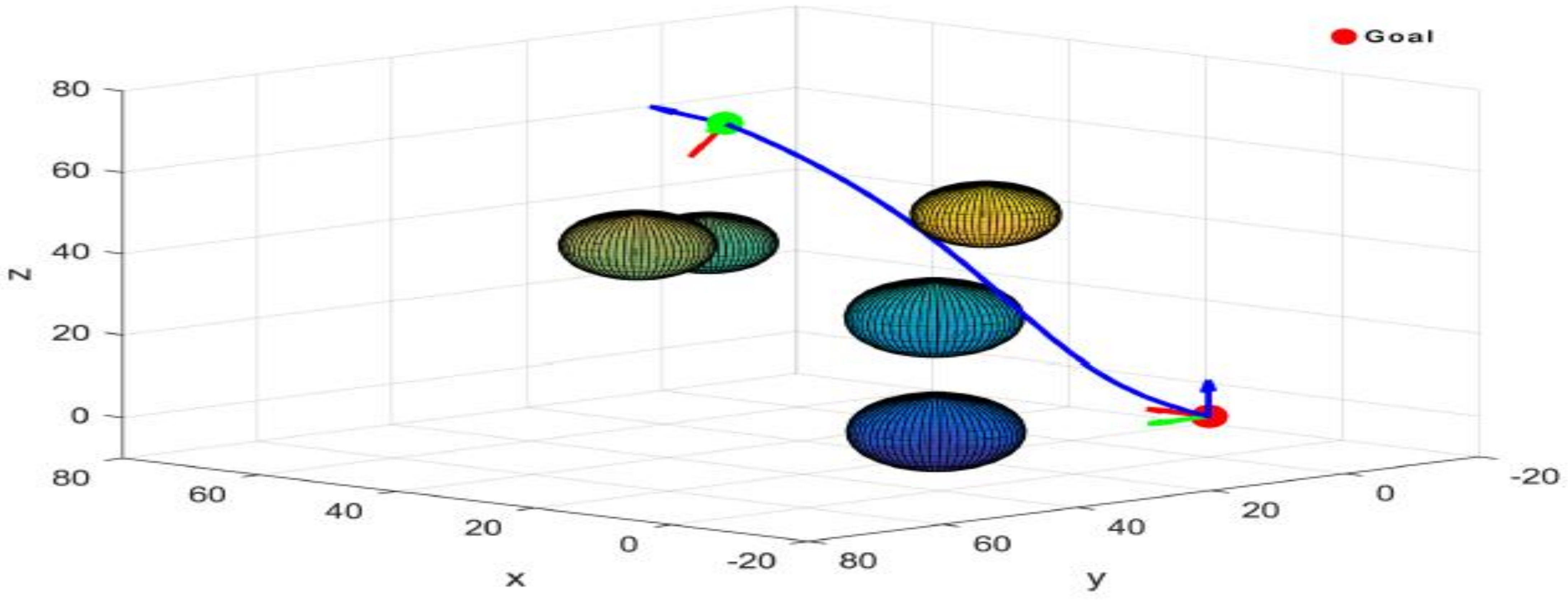

Fig. 5 Illustration of collision-free trajectory of chaser satellite using D-APF

Simulation Results

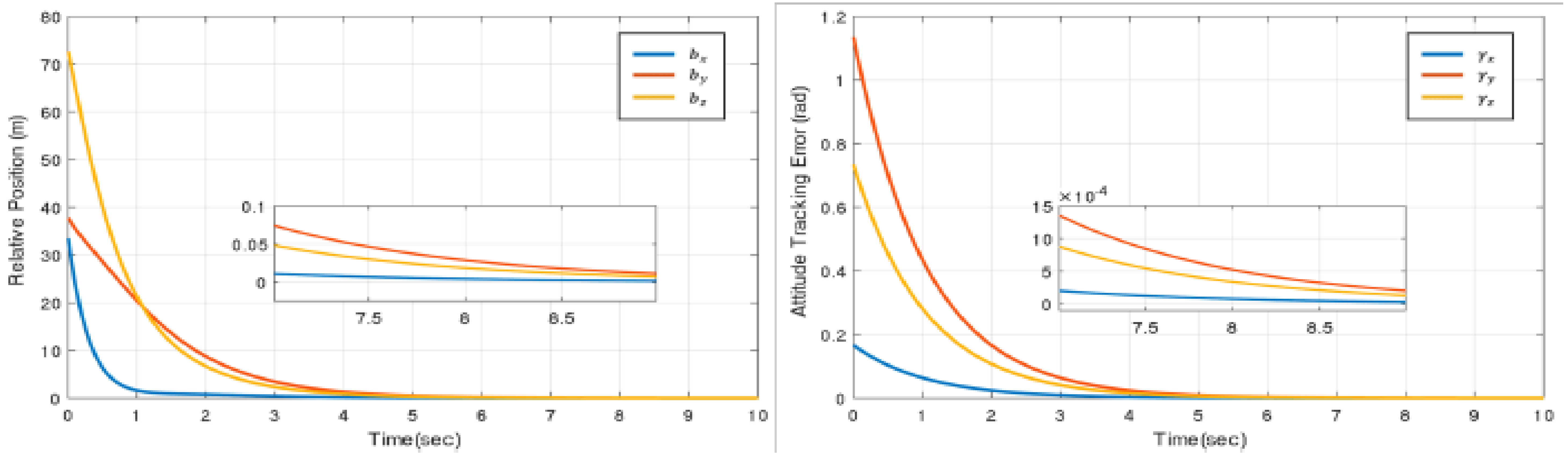

Fig. 6 Plot of Configuration Tracking error (a) Relative Position (left)
(b) Attitude tracking error (right)

Results

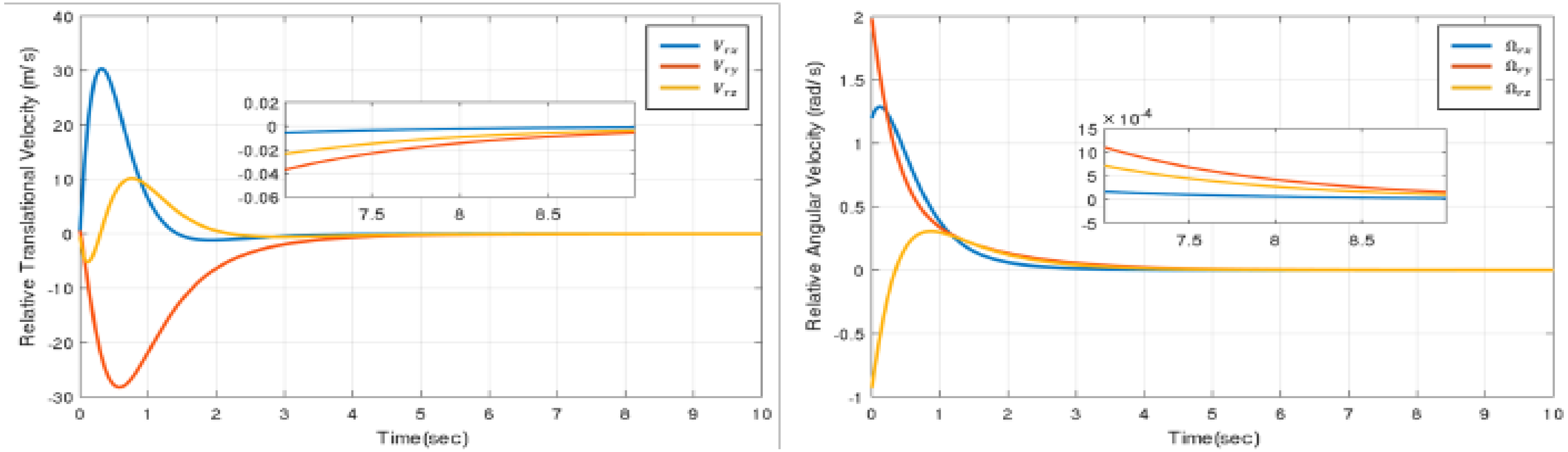

Fig. 7 Plot of Relative Velocity error (a) Translational (left) (b) Rotational (right)

Simulation Results

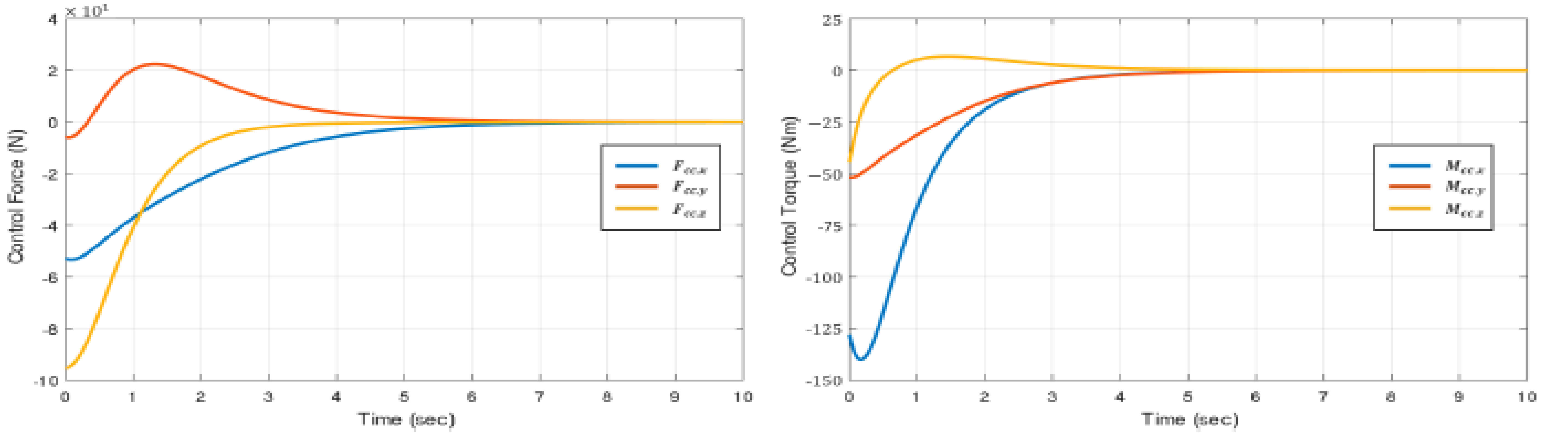

Fig. 8 Plot of Control Input (a) Control Force (left) (b) Control Moment (right)

Thank You